

Selective Tuning of the HOMO–LUMO Gap of Carbazole-Based Donor–Acceptor–Donor Compounds toward Different Emission Colors

Huaqiang Zhang,^[a,b] Xiangjian Wan,^{*[a]} Xiaosong Xue,^[c] Yanqin Li,^[a,b] Ao Yu,^[c] and Yongsheng Chen^{*[a]}

Keywords: Nitrogen heterocycles / Fused-ring systems / Donor–acceptor systems / Molecular electronics / Luminescence

Carbazole-based donor–acceptor compounds with tunable HOMO–LUMO gaps were synthesized by Suzuki and Sonogashira cross-coupling reactions. Their optical and electrochemical properties were fully characterized. The results

show that materials with different emission colors ranging from blue to green to orange could be obtained. The experimental results were also supported by theoretical calculations.

Introduction

Donor–acceptor (D-A)-type conjugated molecules have attracted increasing attention, as they can serve as efficient electroluminescent (EL)^[1,2] and nonlinear optical (NLO) materials.^[3,4] The EL and NLO performances of these molecules are effectively dependent on their HOMO–LUMO or band gaps associated with intramolecular D-A interactions. The strength of D-A interactions is determined by donor and acceptor groups and the connecting π bridges. Strong electron-donating or -accepting groups and short π bridges often enhance D-A interactions, whereas weak electron-donating or -accepting groups and long π bridges lower D-A interactions.^[5] To utilize these characteristics in practical optoelectronic materials, many conjugated polymers based on carbazole, which is a good electron-donating group, have been prepared and their properties were extensively investigated.^[5,6] However, carbazole-based conjugated small molecules of this series have only been scarcely reported. Moreover, arylation at the 9-position of carbazoles leads to a shift in its highest occupied molecular orbital (HOMO) level to lower energy,^[7] and this is helpful to obtain a wider range of band gaps when associated with proper acceptor groups. In this paper, we synthesize a series of new D-A molecules (Scheme 1, compounds **1–4**) composed of carbazole moieties as the donor group and a benzothiadiazole or anthracene moiety as the acceptor part, through phenyl and phenylethynyl conjugated bridges.

Intramolecular D-A interaction of these molecules was investigated by optical absorption and emission spectroscopy as well as electrochemistry. Different emission colors ranging from blue to green to orange were observed for these compounds, and this is consistent with the theoretical calculation results.

Results and Discussion

The synthesis of compounds **1–4** is outlined in Scheme 1. The starting material 3,6-di-*tert*-butyl-9-[4-(4,4,5,5-tetramethyl-1,3,2-dioxaborolan-2-yl)phenyl]-9*H*-carbazole was synthesized according to the literature^[8] and was treated with 9,10-dibromoanthracene^[9] and 4,7-dibromobenzothiadiazole^[10] to obtain **1** and **3** through Suzuki reactions,^[11] respectively. The other starting material, 3,6-di-*tert*-butyl-9-(4-ethynylphenyl)-9*H*-carbazole, was synthesized according to a reported procedure,^[12] which was then subjected to Sonogashira couplings^[13] with 9,10-dibromoanthracene and 4,7-dibromobenzothiadiazole to afford **2** and **3**, respectively. Compounds **1–4** were all readily soluble in common organic solvents such as toluene, dichloromethane, and THF. Their structures and purities were characterized and verified by ¹H and ¹³C NMR spectroscopy and HRMS.

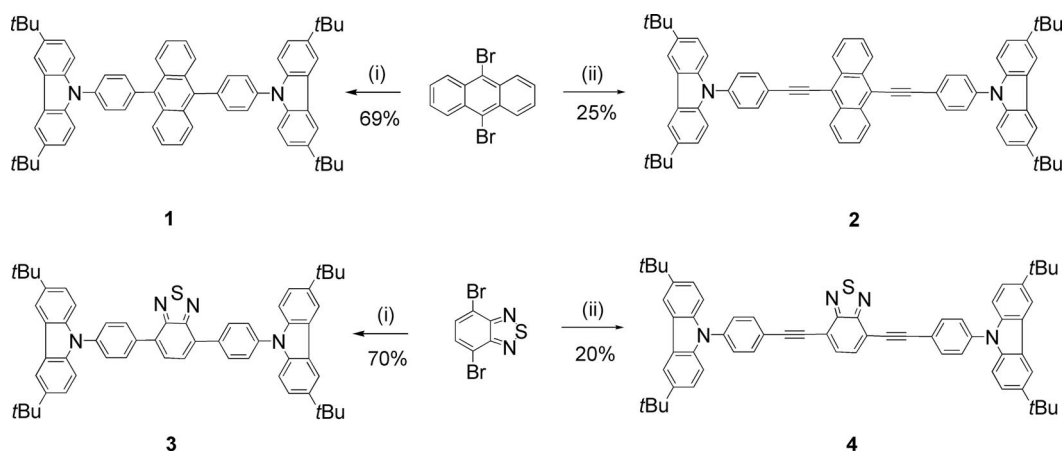
The thermal stabilities of **1–4** were investigated by thermogravimetric analysis (TGA), as shown in Figure 1. The results reveal that the onset decomposition temperatures of the compounds are all around 450 °C under a nitrogen atmosphere, which indicates that they are quite thermally stable and can be used for various high-temperature processes in the construction of electronic devices.

The absorption and emission spectra of **1–4** were measured in dichloromethane, and the relevant data are presented in Table 1. The absorption spectra of **1–4** show intensive transitions in the UV region, with strong absorption bands in the range 200–300 nm (Figure 2, Table 1). The

[a] Key Laboratory for Functional Polymer Materials and Center for Nanoscale Science and Technology, Institute of Polymer Chemistry, Nankai University, Tianjin 300071, China
Fax: +86-22-23499992
E-mail: xjwan@nankai.edu.cn
yschen99@nankai.edu.cn

[b] Lanzhou Petrochemical Research Center, PetroChina, Lanzhou 730060, China

[c] Central laboratory, College of Chemistry, Nankai University, Tianjin, China



Scheme 1. The synthesis of compounds 1–4. Reagents and conditions: (i) 3,6-di-*tert*-butyl-9-[4-(4,4,5,5-tetramethyl-1,3,2-dioxaborolan-2-yl)phenyl]-9*H*-carbazole, Pd(PPh₃)₄, 2 M K₂CO₃ (aq.), PPh₃, aliquat 336, toluene, reflux, 24 h; (ii) 3,6-di-*tert*-butyl-9-(4-ethynylphenyl)-9*H*-carbazole, PdCl₂(PPh₃)₂, CuI, (*i*Pr)₂NH, 80 °C, 24 h.

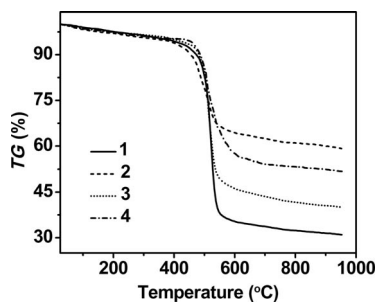


Figure 1. TGA plots of 1–4 with a heating rate of 10 °C min⁻¹ under a N₂ atmosphere.

bands at about 240 and 296 nm for these compounds are assigned to carbazole-centered transitions.^[14] For 1 and 2, peaks at ca. 350–400 nm with characteristic vibronic patterns are attributed to the π – π^* transition of anthracene,^[15] whereas the absorption features of 3 and 4 at wavelengths in the 300–350 nm region show moderately strong absorbances, which are assigned to the π – π^* absorption band of benzothiadiazole.^[16] Apart from the characteristic absorptions of the donors and acceptors, the solution spectra of 1–4 show new broad bands at a longer wavelength of 400–500 nm, which depends on their effective conjugation lengths.^[17] Among the four compounds, 1 exhibits the lowest effective conjugation length for this new band and thus has the shortest effective conjugation length along the molecule, whereas the longest effective conjugation length is observed for 2 from its onset absorption in the ground state. Out-of-plane twisting of the phenyl ring from the central anthracene possibly deteriorates the extended π -conjugation through compound 1,^[18] whereas the longest effective conjugation length of 2 may be due to the coplanar conformation of the anthracene and ethynylene groups, as reported before.^[19] It can be seen from Table 1 that the optical HOMO–LUMO gap of 3 is smaller than that of 1, indicating a greater delocalization of electrons in 3. This result confirms that changing the electron affinity of the acceptors could effectively modulate the HOMO–LUMO gaps of the molecules and that the benzo-

thiadiazole moiety is a stronger electron acceptor than the anthracene moiety; however, this argument fails to explain the similarity of the HOMO–LUMO gaps between 2 and 4, which have anthracene and benzothiadiazole moieties as their acceptors. This phenomenon may be attributed to the greater interaction between the anthracene and ethynylene groups than that between the benzothiadiazole and ethynylene groups.^[19] In addition to the acceptors combined to the donor chromophores, π -bridges are also known to play an important role in determining the conjugation lengths of these compounds.^[20] In this case, insertion of an ethynylene spacer results in longer onset wavelengths of 2 and 4 than those of 1 and 3, indicating longer effective conjugation lengths and smaller HOMO–LUMO gaps of 2 and 4 than those of 1 and 3, respectively. To gain further insight into the photophysical process within these compounds, we investigated their absorption behaviors in different solvents. The absorption spectra in different solvents (not shown) are nearly independent of solvent polarity, which indicates a negligible intramolecular charge-transfer process between donor and acceptor chromophores in the ground states.^[21]

Table 1. Optical properties of 1–4.

	$\lambda_{\max, \text{abs}}$ [nm] ^[a]	$\lambda_{\max, \text{em}}$ [nm] ^[b]	E_g [eV] ^[c]
1	246, 298, 377, 397	440	2.95
2	238, 297, 458, 479	507	2.40
3	244, 298, 347, 415	581	2.57
4	239, 297, 327, 442	607	2.43

[a] Measured in CH₂Cl₂ solution (concentrations 1: 6.6 × 10⁻⁶ M; 2: 5.0 × 10⁻⁶ M; 3: 8.1 × 10⁻⁶ M; 4: 7.8 × 10⁻⁶ M). [b] Measured in CH₂Cl₂ solution (1 × 10⁻⁶ M). [c] Optical HOMO–LUMO gap derived from the onset wavelength of UV/Vis absorption spectra of 1–4.

The maximum emission wavelengths λ_{\max} in dichloromethane for 1–4 are 440, 507, 581, and 607 nm, respectively (Figure 3). Redshifts in the fluorescence spectra were observed, indicating more effective conjugation on going from 1 to 4 in the excited state. A more intuitive redshift in the emission features could be observed during the photograph

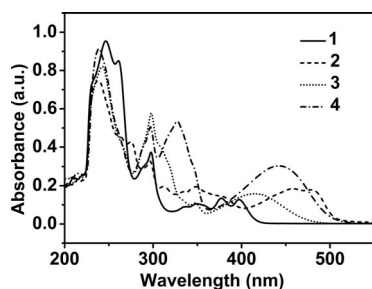


Figure 2. Absorption spectra of **1–4** in degassed dichloromethane (concentrations **1**: 6.6×10^{-6} M; **2**: 5.0×10^{-6} M; **3**: 8.1×10^{-6} M; **4**: 7.8×10^{-6} M, different concentrations were used for the purpose of optimal absorbance).

experiment. When irradiated with UV light at 365 nm, the emission colors of the compounds ranging from blue to green to orange were observed (see graphic in the Table of Contents). Compound **1** and **2** exhibit a featureless emission, displaying normal Stoke shifts of ca. 2589 and 1690 cm^{-1} , which could be assigned to the locally excited singlet π – π^* emissions.^[22] Compounds **3** and **4** are species containing donor (the carbazole moieties) and acceptor (the benzothiadiazole group) subunits and in which rotation of the donor part of the molecule with respect to the acceptor part is allowed. As such, twisted intramolecular charge-transfer (TICT) excited states and luminescence might be observed for **3** and **4**.^[23] This is true and supported by the following results:^[24] (i) The large Stoke shifts of ca. 7059 and 5748 cm^{-1} for **3** and **4**, respectively. (ii) The broad featureless shape of the emission spectra. (iii) The solvent dependence of the emission spectra, as shown in Figure 4 for compound **3** and **4**. For such species, the emission band strongly moves to the red upon increasing the polarity of the solvents from heptane, dioxane, THF, and dichloromethane to MeCN. The emission maximum of **3** and **4** shifted significantly to the longer wavelength region by ca. 100 nm (from 511 nm in heptane to 611 nm in MeCN) along with a decrease in the fluorescence intensity. The decreasing emission with increasing polarity of the solvent is mainly attributed to the lower solubility of **3** and **4** in polar solvents. This can increase the intermolecular vibronic interactions of **3** and **4**, respectively, which induce the nonradiative deactivation process, that is, fluorescence quenching, such as excitonic coupling and excimer forma-

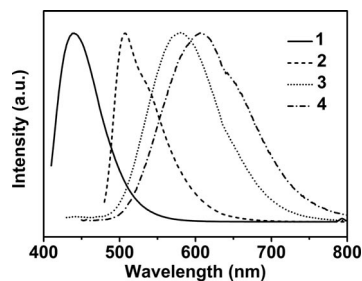


Figure 3. Room-temperature corrected emission profiles of 1×10^{-6} M solutions of **1–4** in dichloromethane (λ_{ex} **1**: 395 nm; **2**: 467 nm; **3**: 412 nm; **4**: 450 nm).

tions.^[25] All the compounds give relatively high fluorescence quantum yields (Φ_{PL}) in dichloromethane solution: 0.6 for **1**, 0.55 for **2**, 0.30 for **3**, and 0.35 for **4** (Rhodamine B as the standard, $\Phi_{\text{PL}} = 0.65$ in ethanol).^[3]

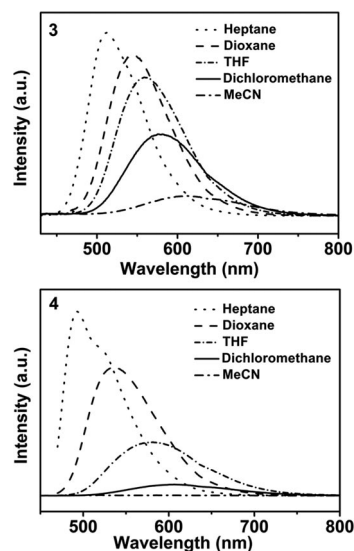


Figure 4. Room-temperature uncorrected emission spectra of **3** and **4** in heptane, dioxane, THF, dichloromethane, and MeCN at 1×10^{-6} M (λ_{ex} **3**: 412 nm; **4**: 450 nm).

The maximum emission wavelengths λ_{max} in thin films of **1–4** are 439, 506, 550, and 557 nm, respectively (Figure 5). The thin film emission spectra of **1** and **2** are similar to those in dichloromethane solution, but obvious blueshifts of the fluorescence emissions for **3** and **4** are observed in thin films compared to those in dichloromethane solutions. The blueshifts can be explained by the fact that in the solid state, compounds **3** and **4** possess a narrower distribution of conformations, which gives rise to a higher energy HOMO–LUMO gap in the excited states.

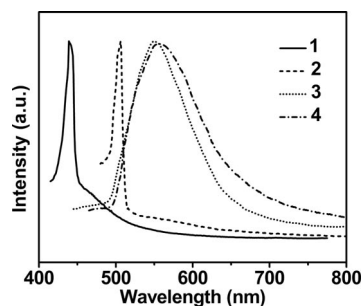


Figure 5. Room-temperature corrected emission spectra of **1, 2, 3**, and **4** recorded in thin films spin-coated from dichloromethane solutions on quartz substrate (λ_{ex} **1**: 400 nm; **2**: 464 nm; **3**: 422 nm; **4**: 450 nm).

The redox properties of **1–4** have been investigated in dichloromethane as shown in Figure 6, and the results are summarized in Table 2. From cyclic voltammetry measurements, compounds **1** and **2** were found to exhibit a single reversible oxidation process at 1.17 and 1.21 V vs. SCE, which could be assigned to simultaneous one-electron oxidation of the two carbazole units.^[26] Such an outcome may

be due to the noncoplanarity of the central anthracene with 9,10-substituents, which results in negligible electronic interactions between the carbazole units.^[18] Similarly for compounds **3** and **4**, there exists a single reversible oxidation process at 1.15 and 1.17 V vs. SCE, which could be also assigned to simultaneous one-electron oxidation of the two carbazole units. Similar results for benzoselenadiazole derivatives have been reported before.^[27] The similarity of the oxidation potentials of **1–4** suggests that the interactions between donor groups (carbazole moieties) and acceptor (benzothiadiazole or anthracene groups) are weak in the ground state. As such, the HOMO energy levels of the four compounds, which come from their onset oxidation potentials, are close to each other. Apart from the oxidation process, compounds **3** and **4** also show a single reversible reduction process at -1.43 and -1.22 V vs. SCE. The reduction potential of **4** shifts positively compared to that of **3** upon insertion of the ethynylene segment into the conjugation bridge. This indicates that the reduction in **4** originates from the diethynylbenzothiadiazole low HOMO–LUMO gap chromophore, whereas in **3**, it originates from the benzothiadiazole segment. Similar observations were reported earlier for the dithienylbenzothiadiazole derivatives.^[2,28] Thus, as shown in Table 2, the relatively smaller HOMO–LUMO gap of **4** compared to that of **3** is ascribed to the much lower lowest unoccupied molecular orbital (LUMO) energy level of **4**. Compounds **3** and **4** both undergo remarkably reversible oxidation and reduction processes, suggesting their potential use for bipolar charge transport properties.^[29] This is also supported by the following theoretical results.

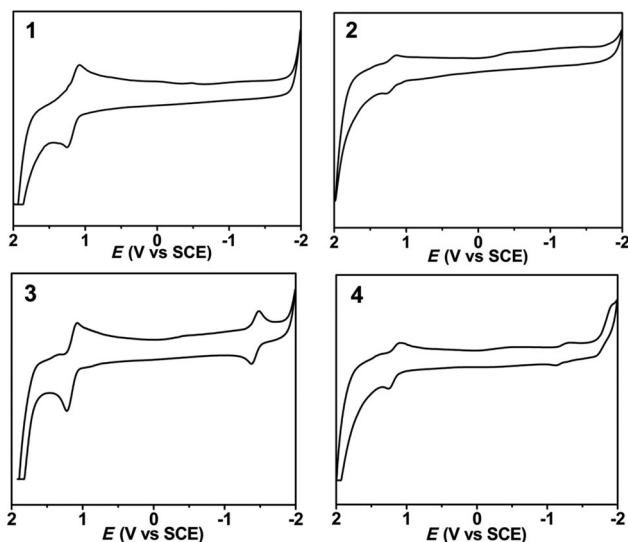


Figure 6. Cyclic voltammograms of **1–4** with a concentration of 0.01 M in 0.1 M Bu₄NPF₆/CH₂Cl₂ with a glassy carbon electrode at a scan rate of 100 mV s⁻¹. A platinum wire and an SCE were used as the counter and reference electrode, respectively.

To provide further evidence for the observed electronic properties of these compounds, theoretical calculations were carried out with the Gaussian 03 packages^[30] on an NK Star Supercomputer by using the B3LYP/6-31G(d)//

Table 2. Electrochemical properties and calculated energy differences of **1–4**.

	Oxidation ^[a] E_{pc}/E_{pa} [V] ^[b]	Reduction ^[a] E_{pc}/E_{pa} [V] ^[b]	HOMO/LUMO ^[c] [eV]	HOMO–LUMO gap ^[d] [eV]
1	1.26/1.08		-5.47/	
2	1.29/1.13		-5.48/	
3	1.22/1.08	-1.38/-1.48	-5.45/-3.08	2.37
4	1.26/1.09	-1.12/-1.33	-5.48/-3.26	2.22

[a] Determined by cyclic voltammetry in CH₂Cl₂ with SCE as a reference electrode. Scan rate of 100 mV s⁻¹. [b] E_{pa} and E_{pc} stand for anodic peak potential and cathodic peak potential, respectively. [c] HOMO/LUMO = $-(E_{onset} + 4.4)$ eV. [d] Cyclic voltammetric HOMO–LUMO gap derived from the difference between HOMO and LUMO energy levels.

AM1/AM1 model, which was shown to be capable of accurately evaluating the ionization potentials (a property of the HOMO) of polysubstituted aromatics.^[31,32] For convenience purposes, the *tert*-butyl groups, which have a minor influence on the electronic properties of the conjugated molecules, were displaced by hydrogen atoms. The geometry of each species was fully optimized at the AM1 level with no symmetry constraints. For the molecules that have more than one possible conformation, the conformation with the lowest electronic energy was singled out and used in the ensuing calculations. Frequency calculations were computed on these geometries at the same level to verify that they are real minimums on the potential energy surface without any imaginary frequency. Subsequently, single-point electronic energy calculation on the optimized geometries were performed at the B3LYP/6-31G(d) level of theory.

The contours of the HOMO and LUMO of the four compounds are shown in Figure 7, from which we can see that the HOMOs of these compounds are delocalized

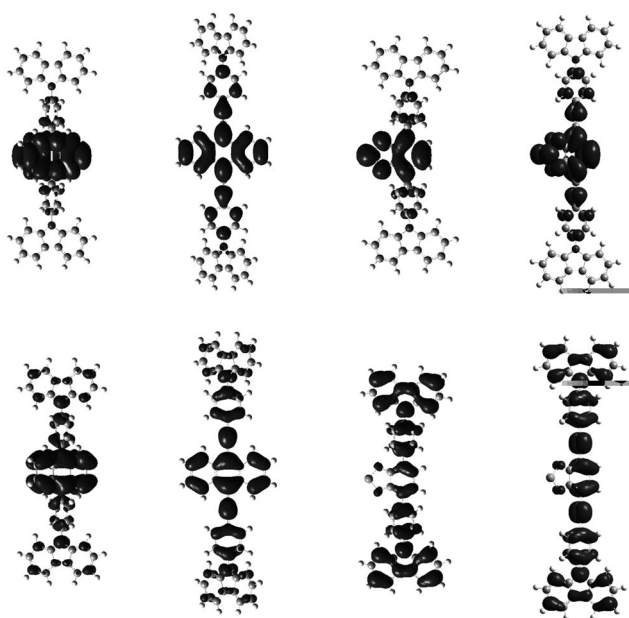


Figure 7. HOMO and LUMO of **1–4** calculated at B3LYP/6-31G(d)//AM1/AM1.

among the whole molecules. The shapes of the HOMOs look very similar to each other for **1** and **2** and for **3** and **4**. The LUMOs of these compounds are delocalized through the acceptors and π bridges. Thus, when the transition occurs from the HOMO to the LUMO by photoexcitation, the LUMO plays an important role in discriminating between the photoluminescence properties of these compounds. The calculated HOMO–LUMO gaps for **1–4** were calculated to be 3.42, 2.50, 2.79, and 2.51 eV, respectively. The calculated results are in good agreement with the experimental values of 2.40–2.95 eV from optical absorption spectra. The difference among the HOMO–LUMO gaps for these compounds is mainly caused by the LUMO energy level. The LUMO energy can be lowered when the LUMO is delocalized over more space,^[32] and this is particularly the case for compound **4**, as seen in Figure 7 and Table 3. In general, the trends of the molecular properties obtained by calculations are in good agreement with the experimental results.

Table 3. Calculated, cyclic voltammetric and optical HOMO–LUMO gap of compounds **1–4**.

	HOMO [eV]	LUMO [eV]	ΔE [eV] ^[a]	E_g^{cv} [eV] ^[b]	E_g^{opt} [eV] ^[c]
1	–5.18	–1.76	3.42	–	2.95
2	–4.86	–2.36	2.50	–	2.40
3	–5.29	–2.50	2.79	2.37	2.57
4	–5.22	–2.71	2.51	2.22	2.43

[a] ΔE calculated at B3LYP/6-31G(d)//AM1/AM1. [b] Cyclic voltammetric HOMO–LUMO gap. [c] Optical HOMO–LUMO gap.

Conclusions

A series of donor–acceptor compounds featuring carbazole moieties as the electron-donating units have been successfully prepared by Suzuki and Sonogashira cross-coupling reactions. The absorption, emission, electrochemical properties, as well as the HOMO–LUMO gaps of these dipolar compounds are significantly affected by the different acceptors and π bridges. Theoretical calculations provided further evidence for the observed electronic properties. Depending on the degree on effective π conjugation within these compounds associated with their HOMO–LUMO gaps, materials **1–4** show redshifted optoelectronic properties with different emission colors ranging from blue to green to orange. Thus, by modifying each part of the D-A molecules, particularly the π bridges, the HOMO–LUMO gaps of these molecules could be tuned in a controlled way. Further work for this tuning, solid fluorescence properties, and the optoelectronic application studies for these molecules are in progress.

Experimental Section

Methods and Materials: Unless stated otherwise, all chemicals and reagents were purchased reagent-grade and used without further purification. Solvents were purified by standard methods. All ma-

nipulations were performed under a dry argon atmosphere by using standard Schlenk techniques. ¹H NMR and ¹³C NMR spectra were recorded with a Bruker AC-300 spectrometer. Chemical shifts, δ , were reported in parts per million relative to the internal standard TMS. Mass spectra (MS) were recorded by using an LCQ Advantage mass spectrometer. High-resolution mass spectra (HRMS) were recorded with a VG ZAB-HS mass spectrometer. Thermogravimetric analysis (TGA) measurement was performed with a TA instrument SDT-TG Q600 under an atmosphere of N₂ at a heating rate of 10 °C min^{–1}. UV spectra were recorded with a JASCO-V570 spectrometer. Cyclic voltammetry (CV) measurements were performed with an LK98B II microcomputer-based electrochemical analyzer at room temperature with a three-electrode cell in a solution of Bu₄NPF₆ (0.1 M) in dichloromethane at a scanning rate of 100 mV s^{–1}. A platinum wire was used as a counter electrode, and an SCE electrode was used as a reference electrode. After measurement the reference electrode was calibrated with ferrocene (Fc). For steady-state luminescence measurements, a Jobin Yvon Horiba spectrometer was used. 3,6-Di-*tert*-butyl-9-[4-(4,4,5,5-tetramethyl-1,3,2-dioxaborolan-2-yl)phenyl]-9*H*-carbazole,^[8] 9,10-dibromoanthracene,^[9] 4,7-dibromobenzo[1,2,5]thiadiazole,^[10] and 3,6-di-*tert*-butyl-9-(4-ethynylphenyl)-9*H*-carbazole^[12] were prepared according to previously reported procedures and showed identical spectroscopic properties to those reported therein.

Compound 1: A solution of 9,10-dibromoanthracene (157.9 mg, 0.47 mmol), 3,6-di-*tert*-butyl-9-[4-(4,4,5,5-tetramethyl-1,3,2-dioxaborolan-2-yl)phenyl]-9*H*-carbazole (500 mg, 1.04 mmol), Pd(PPh₃)₄ (55 mg, 0.05 mmol), aqueous K₂CO₃ (2 M, 6 mL, 11.6 mmol), PPh₃ (40 mg, 0.15 mmol), and aliquat 336 (2 drops) in toluene (30 mL) was heated at reflux for 24 h. The mixture was quenched with water after cooling back to room temperature and extracted with dichloromethane. The combined organic extracts were dried with anhydrous Na₂SO₄ and concentrated by rotary evaporation. The residue was purified by flash chromatography on silica (CH₂Cl₂/hexane, 1:8) to obtain the pure compound as a colorless solid. (289 mg, 69%). ¹H NMR (300 MHz, CDCl₃, TMS): δ = 8.23 (s, 4 H, ArH), 7.93 (dd, J = 3.27, 3.24 Hz, 4 H, ArH), 7.86 (d, J = 8.3 Hz, 4 H, ArH), 7.74 (d, J = 8.3 Hz, 4 H, ArH), 7.66 (d, J = 8.6 Hz, 4 H, ArH), 7.58 (d, J = 8.7 Hz, 4 H, ArH), 7.50 (dd, J = 3.2, 3.2 Hz, 4 H, ArH), 1.53 [s, 36 H, C(CH₃)₃] ppm. ¹³C NMR (75 MHz, CDCl₃): δ = 143.1, 139.3, 137.7, 137.6, 136.5, 132.7, 130.1, 126.9, 126.5, 125.4, 123.7, 123.6, 116.3, 109.4, 34.8, 32.0 ppm. HRMS (MALDI): calcd. for C₆₆H₆₄N₂ [M]⁺ 884.5070; found 884.5061. C₆₆H₆₄N₂ (885.25): calcd. C 89.55, H 7.29, N 3.16; found C 89.49, H 7.33, N 3.20.

Compound 2: A solution of 9,10-dibromoanthracene (168 mg, 0.5 mmol) and 3,6-di-*tert*-butyl-9-(4-ethynylphenyl)-9*H*-carbazole (379 mg, 1 mmol) in diisopropylamine (10 mL) was added to PdCl₂(PPh₃)₂ (70 mg, 0.1 mmol) and copper(I) iodide (19 mg, 0.1 mmol). After the mixture was stirred at 80 °C for 12 h, the reaction mixture was poured into water and extracted with dichloromethane. The combined organic layer was neutralized with 1 N HCl, washed with brine, dried with anhydrous Na₂SO₄, and concentrated by rotary evaporation. The residue was purified by flash chromatography on silica (CH₂Cl₂/hexane, 1:6) to obtain the pure compound as a red solid (117 mg, 25%). ¹H NMR (300 MHz, CDCl₃, TMS): δ = 8.77 (dd, J = 3.3, 3.3 Hz, 4 H, ArH), 8.16 (d, J = 1.3 Hz, 4 H, ArH), 8.01 (d, J = 8.5 Hz, 4 H, ArH), 7.70 (m, 8 H, ArH), 7.52 (dd, J = 8.6, 1.9 Hz, 4 H, ArH), 7.46 (d, J = 8.4 Hz, 4 H, ArH), 1.49 [s, 36 H, C(CH₃)₃] ppm. ¹³C NMR (75 MHz, CDCl₃): δ = 143.4, 143.3, 138.9, 138.7, 138.6, 134.0, 133.1, 132.2, 127.3, 126.9, 126.6, 126.4, 123.8, 123.7, 116.3, 109.2, 34.7, 32.0 ppm. HRMS (MALDI): calcd. for C₇₀H₆₅N₂ [M + H]⁺

933.5148; found 933.5139. $C_{70}H_{64}N_2$ (933.29): calcd. C 90.09, H 6.91, N 3.00; found C 90.03, H 6.96, N 3.01.

Compound 3: A solution of 4,7-dibromobenzo[1,2,5]thiadiazole (111 mg, 0.37 mmol), 3,6-di-*tert*-butyl-9-[4-(4,4,5,5-tetramethyl-1,3,2-dioxaborolan-2-yl)phenyl]-9*H*-carbazole (400 mg, 0.833 mmol), $Pd(PPh_3)_4$ (55 mg, 0.05 mmol), aqueous K_2CO_3 (2 M, 6 mL, 11.6 mmol), PPh_3 (40 mg, 0.15 mmol), and aliquat 336 (2 drops) in toluene (30 mL) was heated at reflux for 24 h. The mixture was quenched with water after cooling back to room temperature and extracted with dichloromethane. The combined organic extract was dried with anhydrous Na_2SO_4 and concentrated by rotary evaporation. The residue was purified by flash chromatography on silica (CH_2Cl_2 /hexane, 1:3) to obtain the pure compound as a light-yellow solid (319 mg, 70%). 1H NMR (300 MHz, $CDCl_3$, TMS): δ = 8.27 (d, J = 8.5 Hz, 4 H, ArH), 8.19 (s, 4 H, ArH), 7.99 (s, 2 H, ArH), 7.80 (d, J = 8.5 Hz, 4 H, ArH), 7.55–7.50 (m, 8 H, ArH), 1.50 [s, 36 H, $C(CH_3)_3$] ppm. ^{13}C NMR (75 MHz, $CDCl_3$): δ = 153.0, 142.0, 138.0, 137.4, 134.6, 131.5, 129.5, 127.2, 125.6, 122.6, 122.5, 115.2, 108.3, 33.7, 31.1 ppm. HRMS (MALDI): calcd. for $C_{58}H_{58}N_4S$ [M]⁺ 842.4382; found 842.4376. $C_{58}H_{58}N_4S$ (843.18): calcd. C 82.62, H 6.93, N 6.64; found C 82.53, H 6.98, N 6.60.

Compound 4: A solution of 4,7-dibromobenzo[1,2,5]thiadiazole (147 mg, 0.5 mmol) and 3,6-di-*tert*-butyl-9-(4-ethynylphenyl)-9*H*-carbazole (379 mg, 1 mmol) in diisopropylamine (10 mL) was added $PdCl_2(PPh_3)_2$ (70 mg, 0.1 mmol) and copper(I) iodide (19 mg, 0.1 mmol). After the mixture was stirred at 80 °C for 12 h, the reaction mixture was poured into water and extracted with dichloromethane. The combined organic layer was neutralized with 1 N HCl, washed with brine, dried with anhydrous Na_2SO_4 , and concentrated by rotary evaporation. The residue was purified by flash chromatography on silica (CH_2Cl_2 /hexane, 1:5) to obtain the pure compound as an orange solid (89 mg, 20%). 1H NMR (300 MHz, $CDCl_3$, TMS): δ = 8.14 (d, J = 8.5 Hz, 4 H, ArH), 7.89 (d, J = 8.4 Hz, 4 H, ArH), 7.87 (s, 2 H, ArH), 7.63 (d, J = 8.4 Hz, 4 H, ArH), 7.49 (dd, J = 8.6, 1.8 Hz, 4 H, ArH), 7.42 (d, J = 8.6 Hz, 4 H, ArH), 1.48 [s, 36 H, $C(CH_3)_3$] ppm. ^{13}C NMR (75 MHz, $CDCl_3$): δ = 154.4, 143.3, 138.9, 138.8, 133.5, 132.4, 126.4, 123.8, 123.7, 120.7, 117.2, 116.4, 109.2, 97.1, 86.1, 34.8, 32.0 ppm. HRMS (MALDI): calcd. for $C_{62}H_{59}N_4S$ [$M + H$]⁺ 891.4460; found 891.4447. $C_{62}H_{59}N_4S$ (891.23): calcd. C 83.56, H 6.56, N 6.29; found C 83.64, H 6.51, N 6.33.

Acknowledgments

We gratefully acknowledge financial support from the National Natural Science Foundation of China (50933003, 50902073, 50903044, 20774047), Ministry of Science and Technology (2006CB932702), and Natural Science Foundation of Tianjin City (07JCYBJC03000, 08JCZDJC25300).

- [1] a) Y. X. Yang, R. T. Farley, T. T. Steckler, E. Sang-Hyun, J. R. Reynolds, K. S. Schanze, J. G. Xue, *Appl. Phys. Lett.* **2008**, 163305; b) C. L. Chiang, S. M. Tseng, C. T. Chen, C. P. Hsu, C. F. Shu, *Adv. Funct. Mater.* **2008**, 18, 248–257; c) H. Y. Fu, H. R. Wu, X. Y. Hou, F. Xiao, B. X. Shao, *Curr. Appl. Phys.* **2007**, 7, 697–701; d) H. Choukri, A. Fischer, S. Forget, S. Chenais, M. C. Castex, B. Geoffroy, D. Ades, A. Siove, *Synth. Met.* **2007**, 157, 198–204; e) J. M. Hancock, A. P. Gifford, Y. Zhu, Y. Lou, S. A. Jenekhe, *Chem. Mater.* **2006**, 18, 4924–4932.
- [2] K. R. J. Thomas, J. T. Lin, M. Velusamy, Y. T. Tao, C. H. Chuen, *Adv. Funct. Mater.* **2004**, 14, 83–90.
- [3] S. Kato, T. Matsumoto, M. Shigeiwa, H. Gorohmaru, S. Maeda, T. Ishi-i, S. Mataka, *Chem. Eur. J.* **2006**, 12, 2303–2317.
- [4] S. Kato, T. Matsumoto, T. Ishi, T. Thiemann, M. Shigeiwa, H. Gorohmaru, S. Maeda, Y. Yamashita, S. Mataka, *Chem. Commun.* **2004**, 2342–2343.
- [5] T. Michinobu, K. Okoshi, H. Sako, H. Kumazawa, K. Shigehara, *Polymer* **2008**, 49, 192–199.
- [6] a) H. N. Yi, R. G. Johnson, A. Iraqi, D. Mohamad, R. Royce, D. G. Lidzey, *Macromol. Rapid Commun.* **2008**, 29, 1804–1809; b) P. Karastatiris, J. A. Mikroyannidis, I. K. Spiliopoulos, *J. Polym. Sci., Part A Polym. Chem.* **2008**, 46, 2367–2378; c) Y. G. Kim, B. C. Thompson, N. Ananthakrishnan, G. Padmanaban, S. Ramakrishnan, J. R. Reynolds, *J. Mater. Res.* **2005**, 20, 3188–3198.
- [7] K. Brunner, A. van Dijken, H. Borner, J. Bastiaansen, N. M. M. Kiggen, B. M. W. Langeveld, *J. Am. Chem. Soc.* **2004**, 126, 6035–6042.
- [8] Y. H. Sun, X. H. Zhu, Z. Chen, Y. Zhang, Y. Cao, *J. Org. Chem.* **2006**, 71, 6281–6284.
- [9] O. Cakmak, R. Erenler, A. Tutar, N. Celik, *J. Org. Chem.* **2006**, 71, 1795–1801.
- [10] B. A. D. Neto, A. S. A. Lopes, G. Ebeling, R. S. Gonçalves, V. E. U. Costa, F. H. Quina, J. Dupont, *Tetrahedron* **2005**, 61, 10975–10982.
- [11] K. T. Wong, H. F. Chen, F. C. Fang, *Org. Lett.* **2006**, 8, 3501–3504.
- [12] Y. Liu, M. Nishiura, Y. Wang, Z. M. Hou, *J. Am. Chem. Soc.* **2006**, 128, 5592–5593.
- [13] K. Sonogashira, Y. Tohda, N. Hagihara, *Tetrahedron Lett.* **1975**, 16, 4467–4470.
- [14] a) R. W. Bigelow, G. E. Johnson, *J. Chem. Phys.* **1977**, 66, 4861–4871; b) N. D. McClenaghan, R. Passalacqua, F. Loiseau, S. Campagna, B. Verheyde, A. Hameurlaine, W. Dehaen, *J. Am. Chem. Soc.* **2003**, 125, 5356–5365.
- [15] I. B. Berlman, *Handbook of Fluorescence Spectra of Aromatic Molecules*, Academic Press, New York, **1971**.
- [16] J. L. Wang, Z. M. Tang, Q. Xiao, Y. G. Ma, J. Pei, *Org. Lett.* **2008**, 10, 4271–4274.
- [17] J. Rissler, *Chem. Phys. Lett.* **2004**, 395, 92–96.
- [18] K. Danel, T. H. Huang, J. T. Lin, Y. T. Tao, C. H. Chuen, *Chem. Mater.* **2002**, 14, 3860–3865.
- [19] M. S. Taylor, T. M. Swager, *Angew. Chem. Int. Ed.* **2007**, 46, 8480–8483.
- [20] a) H. Meier, J. Gerold, H. Kolshorn, W. Baumann, M. Bletz, *Angew. Chem. Int. Ed.* **2002**, 41, 292–295; b) M. Bletz, *Angew. Chem. Int. Ed.* **2005**, 44, 2482–2506.
- [21] C. C. Wu, T. L. Liu, W. Y. Hung, Y. T. Lin, K. T. Wong, R. T. Chen, Y. M. Chen, Y. Y. Chien, *J. Am. Chem. Soc.* **2003**, 125, 3710–3711.
- [22] N. Rajendiran, K. Sivakumar, T. Stalin, *Spectrochim. Acta Part A* **2005**, 62, 991–999.
- [23] M. Klessinger, M. Michl, *Excited States and Photochemistry of Organic Molecules*, VCH, New York, **1995**.
- [24] F. Loiseau, S. Campagna, A. Hameurlaine, W. Dehaen, *J. Am. Chem. Soc.* **2005**, 127, 11352–11363.
- [25] J. B. Birks (Ed.), *Photophysics of Aromatic Molecules*, Wiley, London, **1970**.
- [26] H. Q. Zhang, S. M. Wang, Y. Q. Li, B. Zhang, C. X. Du, X. J. Wan, Y. S. Chen, *Tetrahedron* **2009**, 65, 4455–4463.
- [27] M. Velusamy, K. R. J. Thomas, J. T. Lin, Y. S. Wen, *Tetrahedron Lett.* **2005**, 46, 7647–7651.
- [28] J. M. Raimundo, P. Blanchard, H. Brisset, S. Akoudad, J. Roncali, *Chem. Commun.* **2000**, 939–940.
- [29] X. C. Li, Y. Q. Liu, M. S. Liu, A. K. Y. Jen, *Chem. Mater.* **1999**, 11, 1568–1575.
- [30] M. J. Frisch, G. W. Trucks, H. B. Schlegel, G. E. Scuseria, M. A. Robb, J. R. Cheeseman, J. A. Montgomery Jr., T. Vreven, K. N. Kudin, J. C. Burant, J. M. Millam, S. S. Iyengar, J. Tomasi, V. Barone, B. Mennucci, M. Cossi, G. Scalmani, N. Rega, G. A. Petersson, H. Nakatsuji, M. Hada, M. Ehara, K. Toyota, R. Fukuda, J. Hasegawa, M. Ishida, T. Nakajima, Y. Honda, O. Kitao, H. Nakai, M. Klene, X. Li, J. E. Knox, H. P.

- Hratchian, J. B. Cross, V. Bakken, C. Adamo, J. Jaramillo, R. Gomperts, R. E. Stratmann, O. Yazyev, A. J. Austin, R. Cammi, C. Pomelli, J. W. Ochterski, P. Y. Ayala, K. Morokuma, G. A. Voth, P. Salvador, J. J. Dannenberg, V. G. Zakrzewski, S. Dapprich, A. D. Daniels, M. C. Strain, O. Farkas, D. K. Malick, A. D. Rabuck, K. Raghavachari, J. B. Foresman, J. V. Ortiz, Q. Cui, A. G. Baboul, S. Clifford, J. Cioslowski, B. B. Stefanov, G. Liu, A. Liashenko, P. Piskorz, I. Komaromi, R. L. Martin, D. J. Fox, T. Keith, M. A. Al-Laham, C. Y. Peng, A. Nanayakkara, M. Challacombe, P. M. W. Gill, B. Johnson, W. Chen, M. W. Wong, C. Gonzalez, J. A. Pople, *Gaussian 03*, Revision C.02, Gaussian Inc., Wallingford, CT, **2004**.
- [31] a) G. A. DiLabio, D. A. Pratt, J. S. Wright, *Chem. Phys. Lett.* **1999**, *311*, 215–220; b) G. A. DiLabio, D. A. Pratt, J. S. Wright, *J. Org. Chem.* **2000**, *65*, 2195–2203; c) J. S. Wright, E. R. Johnson, G. A. DiLabio, *J. Am. Chem. Soc.* **2001**, *123*, 1173–1183.
- [32] S. J. Lee, J. S. Park, K. J. Yoon, Y. I. Kim, S. H. Jin, S. K. Kang, Y. S. Gal, S. Kang, J. Y. Lee, J. W. Kang, S. H. Lee, H. D. Park, J. J. Kim, *Adv. Funct. Mater.* **2008**, *18*, 3922–3930.

Received: October 15, 2009

Published Online: February 12, 2010